Topics in Catalysis
https://doi.org/10.1007/s11244-020-01240-z

ORIGINAL PAPER

Photocatalytic Degradation of the Malachite Green Dye with Simulated Solar Light Using TiO_2 Modified with Sn and Eu

D. A. Solís-Casados[1,2] · J. Martínez-Peña[1,3] · S. Hernández-López[4] · L. Escobar-Alarcón[5]

Abstract
This work reports on the synthesis of photocatalysts in thin film form of TiO_2 modified with Sn, Eu as well as Sn and Eu simultaneously. The obtained films were characterized by X-Ray Photoelectron Spectroscopy, Raman Spectroscopy and Ultraviolet–Visible Spectroscopy, in order to obtain information on their chemical composition, vibrational features and optical properties respectively. Chemical composition reveal that the tin content was close to 4 at.%, whereas the europium content was approximately 1 at.%. Raman results show that the unmodified material is crystalline TiO_2 in the anatase phase; the Sn addition promotes the formation of the rutile crystalline phase. Europium incorporation as a novel modifier produces TiO_2 in which a mixture of both crystalline phases coexists. Optical measurements reveal that the band gap energy for all samples remains close to 3.4 eV. The photocatalytic activity was evaluated in the degradation reaction of the Malachite Green dye under simulated solar light. The most relevant result is that photocatalysts containing Sn and Eu show higher photocatalytic activity (60% of MG conversion) than the TiO_2 thin film (28% of MG conversion). The main objective of this work was to investigate the changes produced in the resulting material due to Sn and Eu incorporation as well as try to correlate such changes with the corresponding catalytic activity in terms of the Malachite Green dye conversion degree.

Keywords Photocatalysis · Sol–gel · Thin films · TiO_2

1 Introduction

Water pollution is an undesirable process derived from anthropogenic activities, originated mainly from domestic, industrial and hospital effluents discharged as wastewaters to the environment. These effluents can contain chemical contaminants such as pesticides, herbicides, drugs, dyes, perfluorinated compounds, as well as hormones, hygiene and personal care products, among others. The last are the so-called emerging pollutants that are causing alarm in the worldwide because their negative effects on the human health and possible damage to other living species. Among the water pollutants that have attracted special attention are dyes, because they are widely used in the textile and food industry which discharge polluted water with high amounts of them. Particularly, the malachite green (MG) dye besides being used in the textile and food industry is also employed as a dye in a wide variety of drugs, food, mouthwashes, for tinction of the dental plaque, in textile staining and in aquaculture among others. It is worth noting that MG result a toxic agent to the aquatic flora and fauna even at low concentrations [1].

Several processes have been proposed to eliminate organic pollutants contained in wastewaters such as chemical, microbiological and physical, however, the organic molecules are only transferred from one phase to another making these processes non-attractive. Among the most

✉ D. A. Solís-Casados
solis_casados@yahoo.com.mx

1 Universidad Autónoma del Estado de México, Centro Conjunto de Investigación en Química Sustentable UAEM-UNAM, Toluca, Mexico

2 Personal Académico Adscrito a la Facultad de Química UAEMéx, Toluca, Mexico

3 Programa de posgrado en ciencia de materiales, Facultad de Química, UAEMéx, Toluca, Mexico

4 Laboratorio de Desarrollo y Caracterización de Materiales Avanzados (LIDMA), Facultad de Química, Universidad Autónoma del Estado de México (UAEM), UAEMéx, Toluca, Mexico

5 Departamento de Física, Instituto Nacional de Investigaciones Nucleares, Estado de México, Carretera México-Toluca S/N, la Marquesa, Ocoyoacac C.P.52750, Mexico

Published online: 10 February 2020

promising solutions for the removal of organic molecules polluting wastewaters are the advanced oxidation processes (AOP). The photocatalytic process is an AOP that can take advantage of the sunlight as a source of natural radiation being environmentally friendly without toxic or lethal by-products that can affect aquatic species [2]. The photocatalysts generate oxidation agents as hydroxyl ($OH^{\cdot}$) and hydroperoxyl ($OOH^{\cdot}$) radicals as well as reduction agents as the superoxide ($O_2^{\cdot}$) which are capable to breakdown any organic molecule transforming it in CO_2 and water [3].

Semiconductor materials are used as photocatalysts because as a result of their interaction with light are created electron–hole pairs which produce the oxidizing and reducing radicals. Titanium dioxide (TiO_2) is one of the most studied photocatalyst because of its low cost, availability, high stability in aqueous solution, high resistance to photoinduced decomposition and safety to the environment and human beings. However, TiO_2 has two major disadvantages for this application, firstly, the high recombination rate of the photogenerated electron–hole pairs leads to lower degradation rates of organic molecules; secondly, its relatively large band gap energy, close to 3.2 eV for the anatase phase, does not allow the use of the visible part ($\lambda > 400$ nm) of the sunlight [3]. Several strategies have been proposed to overcome these drawbacks such as the TiO_2 modification with transition metals narrowing its band gap extending the optical absorption to longer wavelengths taking advantage of a greater proportion of the sunlight spectrum for its activation; however, it is important to point out that this not guarantee an increase in the photocatalytic activity because the electron–hole pair recombination can be increased [4]. Another TiO_2 modification to enhance its photocatalytic response has been its coupling with other semiconductors to inhibit the electron–hole recombination, transferring electrons between their conduction bands promoting an increase in the photocatalytic activity [5]. Also, the addition of metals as electron traps to favor the oxidation reaction path forming hydroxyl and hydroperoxyl radicals has been reported [6]. Therefore, the development of sunlight activated coupled photocatalysts is currently of great interest. Tin oxide (SnO_2) has been reported as one of the most attractive photocatalyst due to its unique tetragonal rutile-type structure and band gap energy close to 3.6 eV, which still make it active under the UV component of the sunlight [7, 8]. This material has been studied before due its good reduction potential and low oxidation potential, and in spite of its low photocatalytic activity [9] has the advantage that the Sn atoms can be incorporated into the atomic lattice of the TiO_2, promoting the transformation of anatase to the rutile crystalline phase. It has been reported that mixtures of anatase:rutile behave as coupled semiconductors and show synergetic effects increasing the photocatalytic activity, that is the reason for its use in this work The study of the incorporation of europium atoms as a modifier of the photocatalyst [10] is interesting if it is coupled to the TiO_2 lattice as Eu_2O_3, which has a band gap energy of 4.5 eV, higher than anatase (3.2 eV) and rutile (2.8 eV) TiO_2 phases.

Most of the photocatalysts are used in their powder form because is easier to synthesize them; however, the use of photocatalysts in powder form can result in several drawbacks when are utilized for the degradation of organic pollutants present in aqueous media such as wastewaters. The major problem is the recovery of the photocatalyst from the produced suspension which involves the use of separation techniques being more complicated for nano-sized powders. Another problem is the aggregation of suspended powder which can decrease the photocatalytic activity because particles of greater size decreases the surface area and increases the electron–hole recombination rate. Furthermore, the addition of catalyst powder to the aqueous solution containing the pollutant increases the scattering of light affecting the penetration of light to the complete volume under treatment even if the solution is stirred; furthermore for wavelengths in the UV region of the electromagnetic spectrum a lower volume can be irradiated because its lower penetration depth. In order to overcome these problems, it has been proposed the use of photocatalyst supported on different substrates as thin films which have proven in some cases an improved photocatalytic response with the advantage of use very low amounts of catalyst [11–15].

The main aim of this work is to report the modification of titanium dioxide with Sn, Eu as well as Sn and Eu simultaneously for the degradation of the Malachite Green dye under simulated sunlight irradiation, characterizing the physical properties of the prepared materials trying to correlate them with their photocatalytic performance.

2 Experimental

2.1 TiO_2 Thin Films

Thin films were deposited by the spin coating method spreading the precursor solutions, prepared by the sol–gel technique, onto quartz substrates of 25×25 mm at 3500 rpm using a spin coater KW-4A from Chemat Technology. 1 ml of Titanium isopropoxide ($Ti[OCH(CH_3)_2]_4$, Aldrich 97%, was dispersed by stirring in 10 ml of 2-propanol ($CH_3CHOHCH_3$, Fermont 99.8%) until a sol was formed, afterwards nitric acid (HNO_3, Fermont 70%) was added to promote the formation of a gel-like solution. Thin films were thermally treated at 550, 650 and 750 °C to obtain crystalline TiO_2 thin films, this pure material was used a reference photocatalyst.

2.2 TiO_2–(Sn, Eu) Thin Films

A sol was prepared mixing 10 ml of 2-propanol and 1 ml of titanium isopropoxide under stirring at environmental conditions for 1 h. The precursor solution for the Sn modified TiO_2 (TiO_2–Sn) thin films was prepared by adding Stannic chloride ($SnCl_4$ $5H_2O$, Aldrich) slowly under stirring to the gel-like solution obtained previously; the amount of stannic chloride was determined to give a theoretical amount of 20 wt% of SnO_2. Europium nitrate ($Eu(NO_3)_3$ $5H_2O$, Aldrich) was added under stirring to the TiO_2–Sn precursor solution to obtain theorical amounts as Eu_2O_3 of 10 and 20 wt% in the precursor solution used to deposit the Sn, Eu modified TiO_2 (TiO_2–Sn–Eu) thin films. After that, nitric acid was added drop to drop under slow stirring and then aged for 12 h to induce the condensation step in the sol–gel process, changing the sol to an incipient gel, inhibiting the hydrolysis step as a variant of the sol–gel technique reported elsewhere [16]. Afterwards, the precursor solutions, were deposited onto functionalized quartz substrates (25 × 25 mm × 1 mm), spreading a drop by the spin coating technique depositing layer by layer up to 10 layers to obtain homogeneous thin films. These films were thermally treated at 550, 650 and also 750 °C during 4 h to eliminate the organic residues at a heating rate of 3 °C min^{-1} to obtain the thin film in its crystalline form.

2.3 Thin Film Characterization

To determine the elemental atomic content of Titanium, Tin, Europium and Oxygen in the obtained thin films, X-ray photoelectron spectroscopy (XPS) was utilized quantifying the atomic content using the sensitivity factors of the specsurf software from the narrow spectra acquired with a JPS-9200 spectrometer from JEOL. The adventitious carbon (1s) peak was centered at 285 eV and used as internal standard to compensate for charge effects. XPS was also used to determine the chemical bonding information of the detected elements. To study the structural features of the thin films Raman Spectroscopy (RS) was used, the Raman spectra were acquired using an HR LabRam 800 system equipped with a confocal microscope Olympus BX40. A Nd:YAG laser beam (532 nm) was focused on the sample surface with a 50× objective. Spectra were recorded with a cooled CCD camera, typically an average of 50 accumulations of 10 s was done in order to improve the signal to noise ratio. Transmittance spectra were obtained by UV–Vis Spectroscopy using a Perkin Elmer Lambda 35 spectrophotometer, resolution ± 1 nm; the band gap energy was determined applying the Tauc method from the transmittance spectra [17].

2.4 Photocatalytic Activity

The photocatalytic performance of the obtained thin films was evaluated through the degradation of the Malachite Green (MG) dye as model molecule contained in an aqueous solution (10 µmol l^{-1}). The reaction system was prepared by introducing the thin film (1 cm^2) into a 25 ml of the MG solution, afterwards, the reaction system was stirred in dark condition to establish the adsorption equilibrium between the MG solution and the thin film photocatalyst. Thin films were activated in situ by illuminating them with the light emitted by a solar simulator (Sciencetech SF150 model, class A) with an average intensity of 60 mW cm^{-2}, keeping the distance between the liquid surface and the light source at 15 cm. The MG degradation was followed by the decrease of its characteristic absorption band peaking at 619 nm in the UV–Vis absorbance spectra. The spectra were acquired taking aliquots of 4 ml each 15 min in the first hour of reaction time and afterwards, each 30 min during the second and third hour. Absorbance at each reaction time was correlated with the concentration of the MG solution through a calibration curve traced previously, assuming the mineralization of the organic compound. A non-linear least square data treatment was used to determine the kinetic rate constant considering a pseudo-first order kinetic model from the MG concentration versus reaction time graphs [18]. To get information about reaction routes in the photodegradation reaction, reactive species trapping were added to the reaction system [19–21]. To trap the superoxide radicals ($O_2^{\cdot}$) the p-Benzoquinone (BZQ 0.001M) was used, to blockage the holes (h^+) Triethanolamine (TEOA, 0.01M), to trap the hydroxyl radicals ($OH^{\cdot}$) 2-propanol was added (IPA, 0.02 M). These scavenger type molecules were added into the reaction system containing 25 ml of a solution with 10 µmol L^{-1} of MG. In this case MG degradation was also followed by the intensity decrease of the characteristic absorption UV–Vis band located at 619 nm. The absorbance values were correlated through the same calibration curve.

3 Results

3.1 Thermal Analysis

Thermogravimetric analysis (TGA) and differential scanning calorimetry (DSC) were done to choose annealing temperatures above the temperatures of thin films oxidation. From the thermal analysis of the precursor solution containing Ti, Sn and Eu was observed that thermal decomposition occurs at temperatures close to 509 °C as it is seen in Fig. 1. The first step reveal a 83.33% loss of weight due to organic elimination in solution that occurs from room temperature to approximately 188 °C; a second step shows a 4.4% loss of

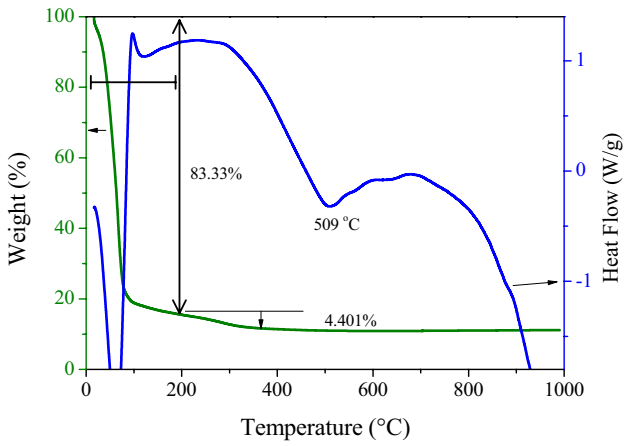

Fig. 1 Thermogravimetric analysis (TGA) and Differential scanning calorimetry (DSC) of the precursor solution of TiO_2–Sn–Eu 20% thin film

weight due to the crystallization of material that occur from 188 to 600 °C with an endothermic peak at 509 °C. From this data it was assumed that precursors in thin films could be completely transformed to the oxidized state at temperatures around 600 °C. Therefore, it was investigated the effect of thermal treatments at 550, 650 and 750 °C on the crystalline structures of thin films and on the catalytic performance of the samples obtained in each case.

3.2 Chemical Composition

Thin films with thicknesses around 55 nm measured by profilometry and mass density close to 25 µgrs cm^{-2} estimated from RBS measurements, were obtained. Due to the very low thickness XPS was used for the compositional characterization because this technique is extremely sensitive to very thin surface layers, typically on the order of 10 to 100 atomic layers and additionally provides information about the oxidation state of the elements present identifying the compounds formed by them.

The chemical composition of the deposited thin films thermally treated at 550 °C is shown in Table 1. It is clearly observed that the TiO_2 thin film without Sn have an atomic composition almost stoichiometric (30 at.% of Ti and 70 at.% of O). Sn and/or Eu incorporation to the thin film gives atomic contents close to 4 at.% Sn and 1 at.% Eu, it seems that stoichiometric ratio has a slight change decreasing Ti to 27 at.% and O to 68 at.%. Chemical composition does not change with the temperature of thermal treatment.

Table 1 Chemical composition of thin films with a thermal treatment of 550 °C

Photocatalyst	(at.%)			
	Ti	Sn	Eu	O
TiO_2	30	0	0	70
TiO_2–Sn	28	5	0	67
TiO_2–Eu	30	0	1	69
TiO_2–Sn–Eu (10%)	26	4	1	69
TiO_2–Sn–Eu (20%)	27	4	1	68

Figure 2 shows the XPS high resolution spectra of the Ti 2p region of the modified TiO_2 thin films. Each spectrum was deconvoluted using Gaussian functions in order to obtain information about the interaction of the Ti with the Sn and O atoms. The deconvoluted spectrum of the TiO_2 thin film thermally treated at 550 °C is shown in Fig. 3a. A doublet is observed with peaks located at 458.8 and 464.5 eV, attributed to the Ti–O interactions in the anatase crystalline phase. Figure 3b shows the Ti region of TiO_2 thin films thermally treated at 650 °C, where three doublets are observed; the first one, with peaks at 457.8 and 461.5 eV, could be attributed to the Ti–O bonds in Ti_2O_3. The presence of Ti^{3+} has been reported before due to oxygen vacancies, result of the transfer of two electrons towards two adjacent Ti^{4+} resulting Ti^{3+} on the surface. Another doublet it is seen at 458.8 and 464.3 eV attributed to Ti–O bonds of the TiO_2 in its anatase phase [22]. A third doublet is seen located at 459.6 y 465.4 eV that can be attributed to the Ti–O bonds assigned to the rutile crystalline phase.As can be seen in Fig. 3c the Ti region of TiO_2 thin films thermally treated at 750 °C, shows the same three doublets with a slight shift, the first one with peaks located at 457.7 and 461.7 eV, could be attributed to the doublet of Ti–O bonds in Ti_2O_3. Another doublet located at 458.7 and 464.2 eV is attributed to the Ti–O bonds of the TiO_2 in its anatase phase [22]. A third doublet is seen at 459.5 y 465.4 eV that can be assigned to

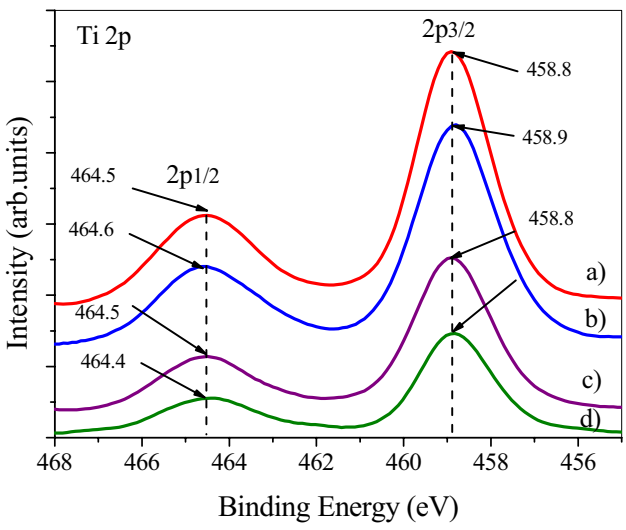

Fig. 2 XPS spectra of Ti 2p region, **a** TiO_2, **b** TiO_2–Sn, **b** TiO_2–Sn–Eu 10%, and **d** TiO_2–Sn–Eu 20%

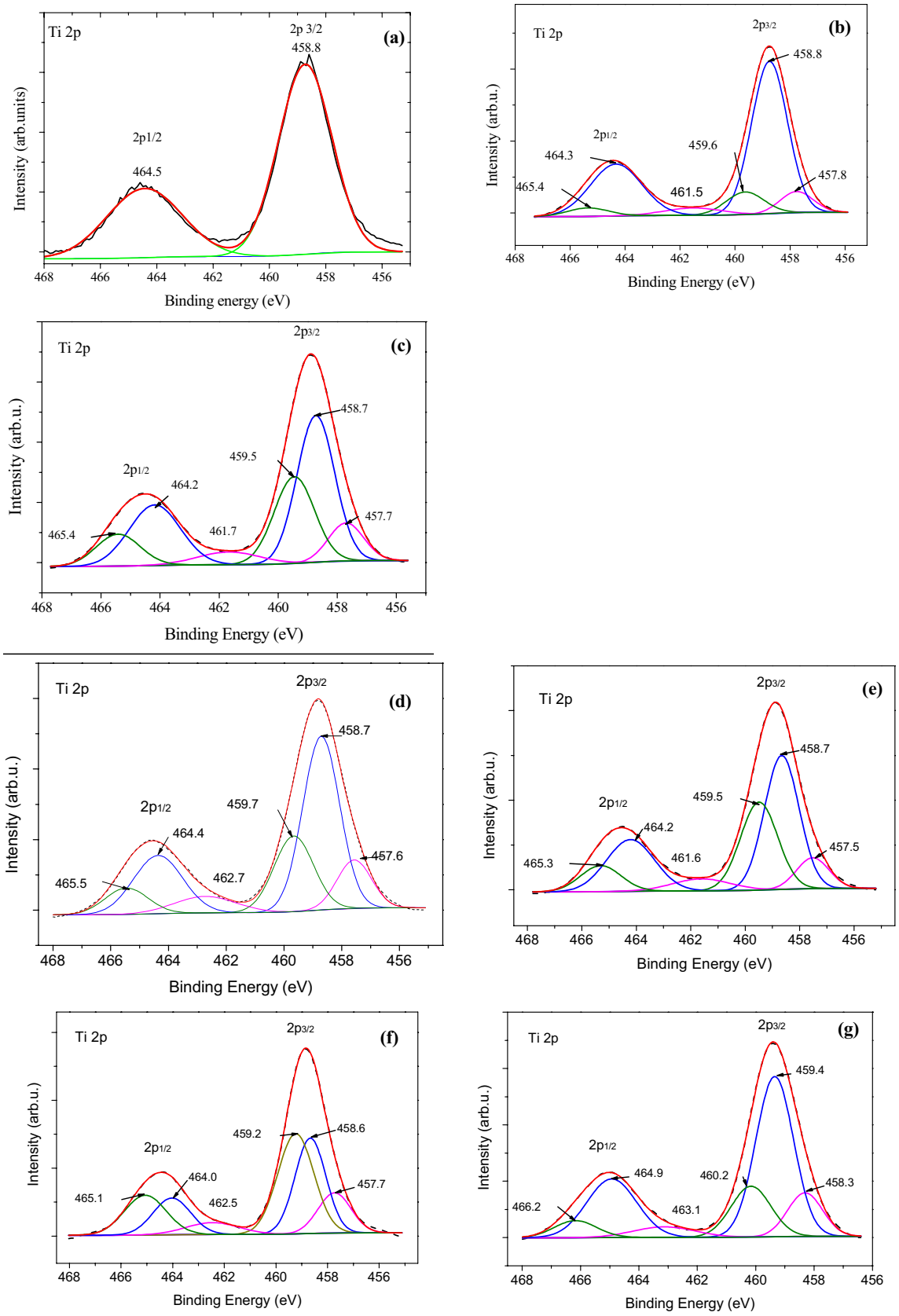

Fig. 3 Gaussian deconvolution of the XPS spectra Ti 2p region **a** TiO_2 550 °C, **b** TiO_2 650 °C, and thin films treated at 750 °C, **c** TiO_2, **d** TiO2–Sn, **e** TiO_2–Sn–Eu 10%, **f** TiO_2–Sn–Eu 20%, and **g** TiO_2–Eu

the Ti–O bonds of the rutile crystalline phase, which was expected since the temperature of thermal treatment was above the temperature of crystalline transition.

The Sn addition in the catalytic formulation change the chemical environment of the Ti, since the thin film has two crystalline phases anatase and rutile, and the crystalline transition occurs at temperatures lower than the expected, because of the Sn incorporation in the atomic structure. The doublet located at 457.6, and 462.7 eV could be attributed to the doublet of Ti–O bonds in Ti_2O_3 (Fig. 3d). Another doublet can be seen at 458.7 and 464.4 eV attributed to Ti–O bonds of the TiO_2 in its anatase phase [22]. A third doublet at 459.7 y 465.5 eV that can be attributed to the rutile crystalline phase in this case due to the Sn incorporation to the atomic structure. After Eu incorporation to the catalytic formulation the spectra of the Ti region shows the same three doublets located in 457.7 and 462.5 eV, the second at 458.6 and 464 eV and the third one at 459.2 and 465.1 eV, suggesting that the Eu is not incorporated into the TiO_2 lattice remaining outside of the crystalline structure as a mixture of $Eu(OH)_3$ or Eu_2O_3 depending of the temperature of thermal treatment. In Fig. 4a–d) are shown the spectra of the Eu region. Figure 4a) shows the spectrum of the Eu_2O_3 sample, that was used as a reference, showing a doublet at 1138.7 and 1168.3 eV; also the Eu 3d region was analyzed and their Gaussian deconvolution is shown in order to stablish if there is any change in the chemical environment of the thin film with the Eu incorporation (Fig. 5a–c).

3.3 Raman Spectroscopy

Micro-Raman spectroscopy was used to identify the crystalline phases present in each sample. It is worth mentioning

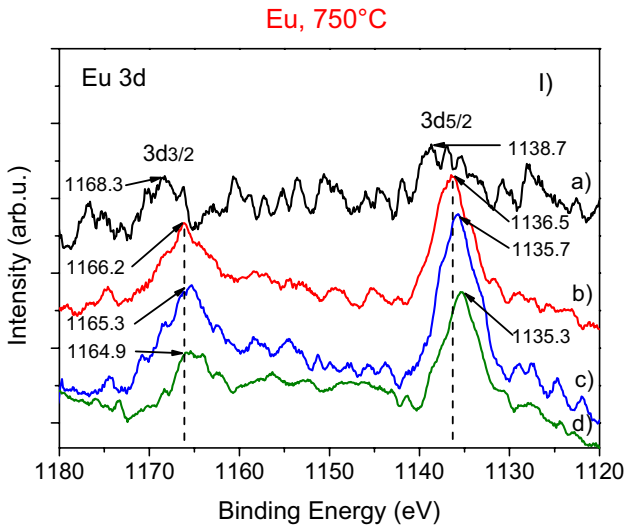

Fig. 4 XPS spectra, thin films treated at 750 °C Eu 3d region

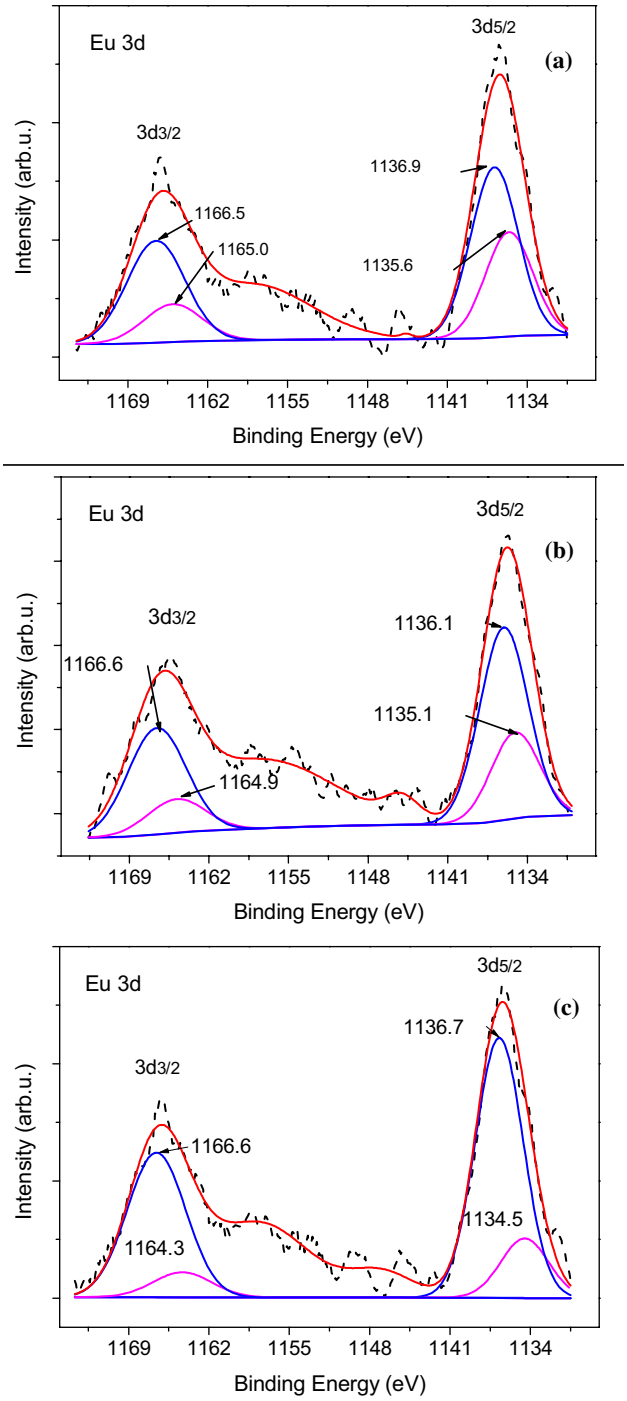

Fig. 5 Gaussian deconvolution of the XPS spectra, thin films treated at 750 °C Eu 3d region, **a** TiO_2–Eu, **b** TiO_2–Sn–Eu 10%, and **c** TiO_2–Sn–Eu 20%

that micro-Raman spectroscopy has been widely used for structural characterization of TiO_2 thin films because its capability to distinguish their different polymorphs, anatase, rutile and brookite [23], being possible even to determine from the Raman spectra the fraction of anatase and rutile that compose a thin film [24]. It must be pointed out that

the complete crystallographic characterization cannot be obtained only from Raman spectroscopy; however, for our purposes it is enough with the micro-Raman characterization. Figure 6a shows the spectra of TiO_2 at different temperatures of thermal treatment. All spectra exhibit Raman bands at 144, 195, 394, 514 and 638 cm^{-1} that are attributed to the anatase crystalline phase [25]. At temperatures of thermal treatment of 650 and 750 °C two small signals appear at 437 and 607 cm^{-1} as the deconvolution of this spectrum reveal in Fig. 2b, which are attributed to the rutile crystalline phase [23]. Therefore, at higher temperatures the films are formed by a mixture of the anatase and rutile phases.

Figure 7I) shows the Raman spectra of the different films subjected to a thermal treatment of 750 °C. As was discussed before the sample of only TiO_2 consist mainly of the anatase phase with a fraction of rutile. To determine the fraction of each crystalline phase from Raman spectra, it was followed the procedure proposed by Clegg [24]. This method employs the ratio of the intensities of the anatase respect to the rutile bands (A_I/I_R) which is linearly related to the anatase/rutile mass ratio (W_A/W_R) through a calibration curve obtained from mixtures of known anatase to rutile fractions. The obtained results, shown in Table 2, indicate a mixture of phases with 21% of rutile and 78% of anatase. For the film with tin it is seen only the presence of the characteristic features of the rutile phase at 143, 444 and 608 cm^{-1}. Therefore, Sn addition promotes the transition from the anatase phase to the rutile phase consistent with previous works [25, 26]. Incorporation of europium preserves the anatase structure as the peak at 143 cm^{-1} indicates, however the spectrum shows a wide band from 250 to 550 cm^{-1} which is shown in detail in Fig. 3II. This band was deconvoluted with peaks at 299, 353, 397, 438, 489 and 517 cm^{-1}. The signals at 397 and 517 cm^{-1} correspond to the anatase phase whereas the peak at 438 can be assigned to the rutile phase; the two Raman peaks found at 299 and 489 cm^{-1} can be attributed to $Eu(OH)_3$ and the band at 353 cm^{-1} suggest the formation of Eu_2O_3 [27]. Therefore, the addition of Eu produces a mixture of the

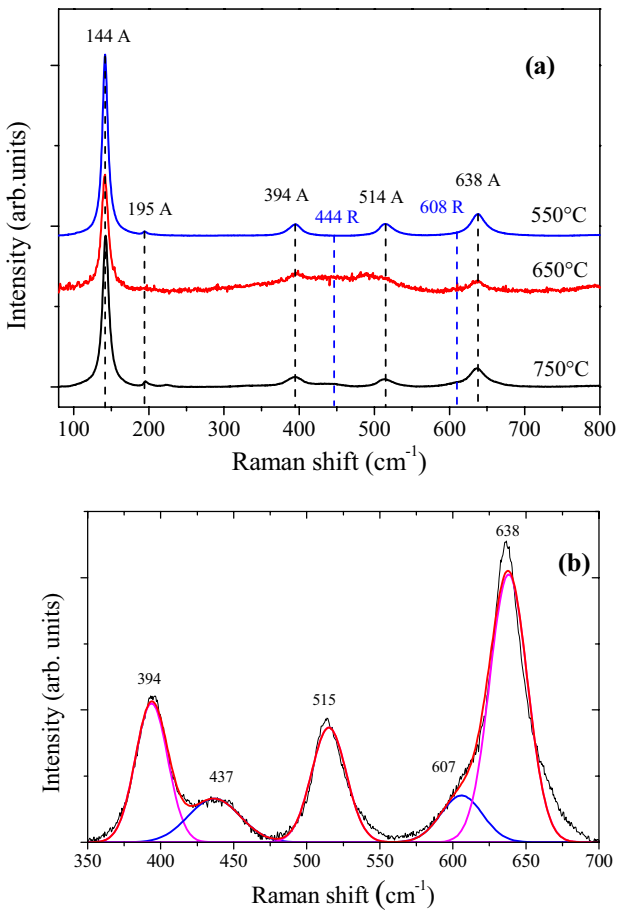

Fig. 6 Raman spectra of TiO_2 **a** thermally treated at 550, 650 and 750 °C, **b** Deconvoluted TiO_2 spectra thermally treated at 750 °C

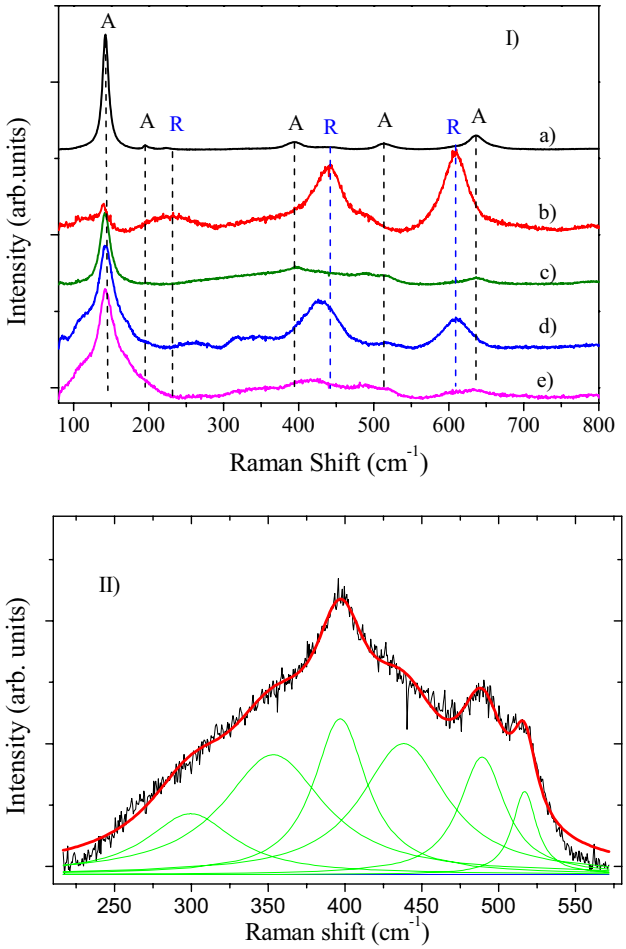

Fig. 7 **I** Raman spectra of the thin films annealed at 750 °C *a* TiO_2, *b* TiO_2–Sn, *c* TiO_2–Sn–Eu 10%, *d* TiO_2–Sn–Eu 20% and *e* TiO_2–Eu 20%. **II** Deconvolution of 225–575 cm^{-1} region in Raman spectra of TiO_2–Sn–Eu 20%

Table 2 Percentages of the crystalline phases, anatase and rutile, determined from the Raman spectra

Photocatalyst	550 °C		650 °C		750 °C	
	A	R	A	R	A	R
TiO_2	100	0	62	38	76	24
TiO_2–Sn	62	38	22	78	0	100
TiO_2–Sn–Eu 10%	53	47	29	71	11	89
TiO_2–Sn–Eu 20%	–	–	21	79	47	53
TiO_2–Eu	100	0	43	57	61	39

Table 3 Band gap energy of the thin films subjected to thermal treatment at different temperatures determined by the Tauc method

Photocatalyst	Band gap energy (eV)		
	550 °C	650 °C	750 °C
TiO_2	3.44	3.46	3.43
TiO_2–Sn	3.44	3.46	3.48
TiO_2–Eu	3.45	3.45	3.43
TiO_2–Sn–Eu 10%	3.38	3.42	3.40
TiO_2–Sn–Eu 20%	3.42	3.41	3.41

anatase (47%) and the rutile (53%) phases of TiO_2 coexisting with $Eu(OH)_3$ and probably Eu_2O_3. The Raman spectrum of the film containing Sn and Eu 10%, reveal clearly the anatase-rutile mixture, in this case the corresponding fractions are 11 and 89% respectively. Finally, the spectrum of the film containing Sn and Eu 20%, resembles the spectrum of the film with Eu, with a mixture 50–50% of the anatase and rutile phases. It is worth noting that for this sample the peak at 143 cm^{-1} becomes wider indicative of distortion of the TiO_2 lattice due to the simultaneous incorporation of Sn and Eu. Additionally, this film seems to contain also $Eu(OH)_3$ and probably Eu_2O_3.

3.4 UV–Vis Spectroscopy

Table 3 shows the optical band gap (Eg) values determined from the transmittance spectra using the Tauc method [17]. This was done by plotting $(\alpha h\nu)^2$ as a function of $h\nu$. The optical absorption coefficient was obtained by $\alpha = -\ln(T)/t$, where t is the thickness of the film and T the transmittance. It seems that there is no change in the band gap energy obtained with Sn addition, which maintains close to 3.44 eV, even with Eu incorporation. It is seen in Table 3 a slight decrease in band gap energy values, in thin films modified with both Sn and Eu, the band gap energy is close to 3.38 eV in thin film with 10% Eu and 3.42 eV in thin film with 20% Eu. It can be considered that there is no change in band gap energy as an effect of the increase in temperature of the thermal treatment provided to the thin films.

3.5 Photocatalytic Activity of Thin Films

Figure 8a–c shows the Malachite Green degradation degree as a function of the reaction time using the obtained thin films thermally treated at 550, 650 and 750 °C under simulated sunlight irradiation. The MG conversion reached in the photolysis process was included for comparison purposes in each case, this uncatalyzed process reached the lowest degradation degree, about 26% after 180 minutes of reaction time. The catalytic activity of the thin films thermally treated at 550 °C show that TiO_2 exhibit a similar tendency as the photolysis process reaching a 32% of MG degradation (Fig. 8a), slightly higher than photolysis, that could be attributed to the fact that this thin film is formed only of the anatase crystalline phase. Thin film containing tin exhibit a better photocatalytic activity than pure TiO_2 attaining a maximum MG conversion close 36.6% after 180 min of reaction time. It is worth noting that this films contains a mixture of anatase:rutile in a ratio of 62:38 which can explain this increase of 14% of the degradation degree. Thin film with 10 at. % of Europium with a ratio 53:47 of anatase:rutile phases shows an improved catalytic activity close to 51.5% after 180 min of reaction time. Further increase of Europium content decrease the MG conversion to 29.7%, probably due to the $Eu(NO_3)_3$ residue because of the low temperature of thermal treatment and found from XPS analysis.

The results of the catalytic tests of the thin films thermally treated at 650 °C (Fig. 8b), show almost the same behavior than the film treated at 550 °C. A higher MG conversion with the Ti–Sn–Eu20% film close to 60%, attributed to the 21:79 mixture of anatase:rutile phases. Film thermally treated at the highest temperature, 750 °C, show a lower MG degradation as is observed in Fig. 8c). This can be due to the high proportion of the rutile phase present in these films as is the case of the TiO_2–Sn film completely formed by the rutile crystalline phase. Table 4 shows the reaction rate constant values, k_{app} (min^{-1}), obtained from fittings of the dye concentration versus reaction time assuming a pseudo first-order expression (exponential curve) using a non-linear least square data treatment with an acceptable precision [18]; Further studies are underway to determine the effect of the Eu incorporation on the reaction route.

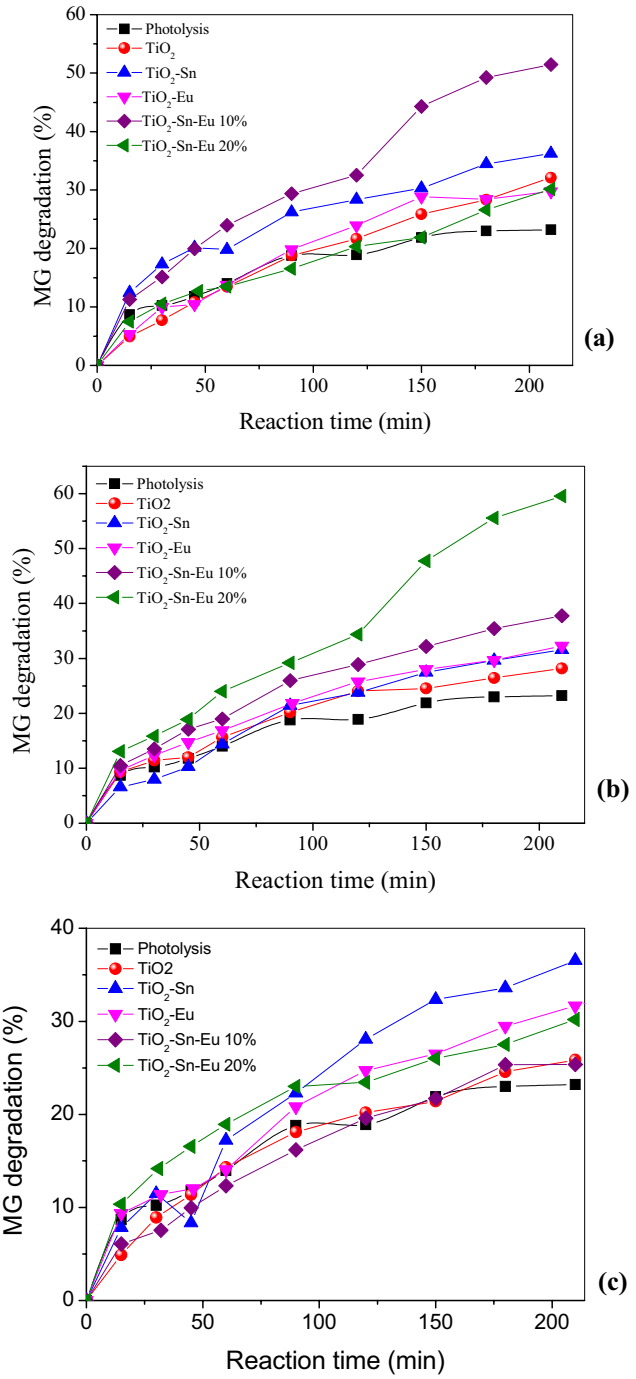

Fig. 8 Photocatalytic activity of thin films annealing at **a** 550 °C, **b** 650 °C and **c** 750 °C

In order to investigate if the obtained degradation values, from 20 to 60%, represent any advantage when thin films are used, degradation tests were performed using 5 mg of TiO_2 Degussa P25, a well-known photocatalyst with high photoactivity. The obtained values reveal a substantially higher photocatalytic activity close to 96% after 90 min of irradiation compared with the maximum degradation degree close to 60% reached by the TiO_2–Sn–Eu 20% thin film after 90 min of irradiation. However, it must be pointed out that in this last case the mass of the thin film employed as photocatalyst, estimated from RBS measurements, was of the order of 25 μgrs; this is equivalent to a dose of 1×10^{-3} g L^{-1}. These results prove that the efficiency demonstrated by the prepared photocatalysts under simulated sunlight irradiation allows an important improvement of the photocatalytic response due to the use of approximately 200 times less mass of photocatalyst and additionally without the problem of the recovery process of the P25 powders.

Table 4 Kinetic rate constants of MG degradation using catalytic formulations thermally treated at different temperatures

k (min^{-1})			
Photocatalyst	550 °C	650 °C	750 °C
TiO_2	0.0016	0.0013	0.0012
TiO_2–Sn	0.0016	0.0016	0.0019
TiO_2–Eu	0.0015	0.0015	0.0015
TiO_2–Sn–Eu (10%)	0.0030	0.0019	0.0012
TiO_2–Sn–Eu (20%)	0.0013	0.0036	0.0013

The photocatalytic degradation route was investigated using scavenger-type molecules based on results reported elsewhere [19–21]. In order to determine the role that the different reactive radicals play in the photodegradation process, the following scavenger were used: Triethanolamine (TEOA) as trap of the photogenerated holes (h^+), p-Benzoquinone (BZQ) for the superoxide radicals ($O_2^{\cdot}$) and 2-Propanol (IPA) for the hydroxyl radicals ($OH^{\cdot}$). It is important to remark that as a function of the photocatalytic material as well as the molecule to be degraded, another kind of scavenger molecules can be used [19–21]. Figure 9

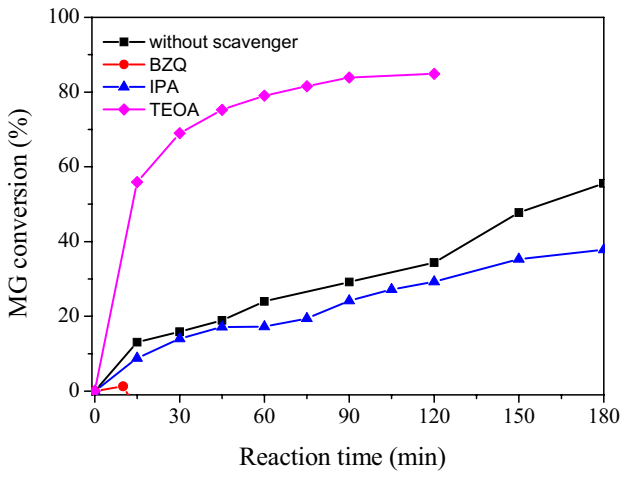

Fig. 9 Photocatalytic activity of TiO_2–Sn–Eu (20%) thin film annealing at 650 °C using scavenger-type molecules

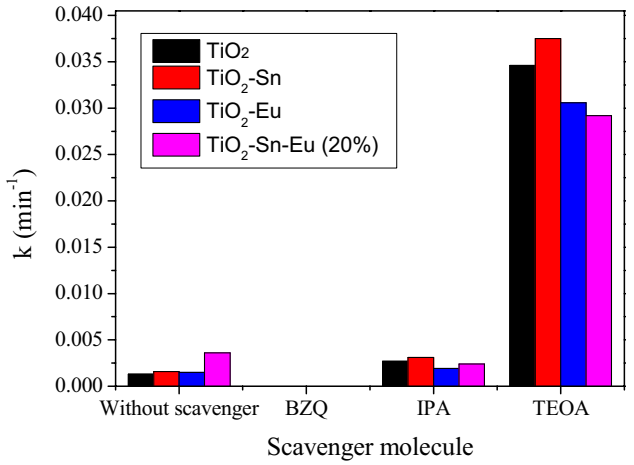

Fig. 10 Kinetic rate constants obtained in MG degradation using scavenger-type molecules

shows the obtained results of photocatalytic activity using the TiO_2–Sn–Eu (20%) thin film annealed at 650 °C. The addition of IPA as scavenger of the $OH^{\cdot}$ results in a MG conversion very similar for reaction times minor than 120 min, approximately 5% lower than the obtained without scavenger suggesting that the hydroxyl radicals practically do not contribute to the MG degradation; however, at reaction times of 180 minutes this difference becomes important, close to 20%, indicating a minor contribution of the $OH^{\cdot}$ radicals in the degradation process. The use of the TEOA scavenger increases significantly the MG conversion reaching 80% after 60 min of reaction, almost 3.3 times the conversion reached without scavenger. This result indicates that the reduction route, initiated by the production of $O_2^{\cdot}$ radicals by the photogenerated e^-, is the responsible of the MG degradation. This was corroborated with the addition of BZQ as $O_2^{\cdot}$ scavenger molecule, whose results show the complete inhibition of the MG photodegradation reaction. Figure 10 shows the kinetic rate constants of the different photocatalysts when reactions are performed in presence of the different scavengers. It is evident that the reduction route is preferred to degrade the MG dye no matter which photocatalyst is used. In this graph is important to remark that the photocatalyst TiO_2–Sn increases the degradation in a great proportion when h + and also when $OH^{\cdot}$ radicals are trapped; the photocatalysts containing Sn or Eu depend in a minor grade of the absence of h + and $OH^{\cdot}$radicals. Even when the preferred route is the reduction one, the photocatalyst TiO_2–Sn–Eu (20%) shows a little change in the catalytic response with the absence of $OH^{\cdot}$ radicals, where was observed a slight decrease in MG degradation respect to the reaction without IPA scavenger, giving the idea that in this particular case $OH^{\cdot}$ radicals also contribute to the degradation reaction through oxidation route even when the main responsible are the $O_2^{\cdot}$ radicals generated through the reduction route. It is assumed that photocatalyst is susceptible to be optimized.

4 Conclusions

TiO_2 photocatalytic formulations containing Sn and Eu in thin film form were obtained. Photocatalysts in thin film form have some advantages compared with catalyst in powder form as an easy way to remove them from the reaction system because are supported on glass substrates as well as the very low amount of photocatalyst utilized. The good catalytic performance (MG conversion of 60%) obtained using amounts as low as 25 µgrs of the catalytic formulation TiO_2–Sn–Eu 20% thermally treated at 650 °C was attributed to the mixture of the anatase-rutile crystalline phases in a ratio 21:79. The use of scavengers allowed to establish that the reduction route drives the MG degradation process no matter which photocatalyst is used. Crystalline phase of rutile can be promoted with the Sn addition and it seems that this transformation can be modulated with the Eu incorporation into the catalytic formulation as can be seen from anatase rutile proportions obtained from Raman spectroscopy.

Acknowledgements Authors thanks to SIEA UAEM 4978/2020CIB Project; To COMECyT for the Grant 19PP1614. Thanks to Dr. Uvaldo Hernández Balderas, M en C Alejandra Núñez, M en C Lizbeth Triana, Dra. Melina Tapia and LIA Citlalit Martinez Soto for technical assistance

Compliance with Ethical Standards

Conflict of interest The authors declare that there is no conflict of interest.

References

1. Srivastava S, Sinha R, Roy D (2004) Aquat Toxicol 66:319–329
2. Chong MN, Jin B, Chow CWK, Saint C (2010) Water Res 44:2997–3027
3. Akpan UG, Hameed BH (2009) J Hazard Mater 170:520–529
4. Chang S, Liu W (2014) Appl Catal B 156–157:466–475
5. Gouvea CAK, Wypych F, Morales SG, Duran N, Nagata N, Peralta-Zamora P (2000) Chemosphere 40:433–440
6. Anthoula C, Papageorgiou NS, Beglitis CL, Pang G, Teobaldi G, Cabailh Q, Chen AJ, Fisher WA, Hofer, Thornton G (2010) Proc Natl Acad Sci USA 107:6 2391–2396
7. Rawal SB, Bera S, Lee D, Jang D, Lee W (2013) Catal Sci Technol 3:1822–1830
8. Batzill M, Diebold U (2005) Prog Surf Sci 79:47–154
9. Ollis DF, Pelizzetti E, Serpone N (1991) Environ Sci Technol 15B:25–29
10. Xu X, Wen S, Mao Q, Feng Y (2019) J Alloy Compd 773:927–933
11. Pérez-Alvarez J, Solís-Casados DA, Romero S, Escobar-Alarcón L (2014) Adv Mater Res 976:212–216

12. Escobar-Alarcón L, Solís-Casados DA, Romero S, Morales-Mendez JG, Haro-Poniatowski E (2014) Appl Phys A 117:31–35
13. Olvera-Rodríguez I, Hernández R, Medel A, Guzmán C, Escobar-Alarcón L, Brillas E, Sirés I, Esquivel K (2019) Sep Purif Technol 224:189–198
14. Pant B, Park M, Park SJ (2019) Coatings 9:613
15. Ahmadi N, Nemati A, Solati-Hashjin M (2014) Mater Sci Semicond Process 26:41–48
16. Solís-Casados D, Escobar-Alarcón L, Fernández M, Valencia F (2013) Fuel 110:17–22
17. Tauc J, Grigorovici R, Vancu A (1966) Phys Status Solidi 15:627
18. Lente G (2015) Deterministic kinetics in chemistry and systems biology Springer, ISBN 978-3-319-15481-7, pp 52–58
19. Difa X, Bei Ch, Shaowen C, Jiaguo Y (2015) Appl Catal B 164:380
20. Lei X, Yongge W, Wan G, Yihang G, Yingna G (2015) Appl Surf Sci 332:682
21. Si-Zhan Wu K, Li W-D, Zhang (2015) Appl Surf Sci 324:324
22. Jovalekic C, Zdujic M, Atanasoska LJ (2009) J Alloys Compds 469:441–444
23. Haro-Poniatowski E, Rodríguez Talavera R, de la Cruz Heredia M, Cano-Corona O, Arroyo-Murillo R (1994) J Mater Res 9:2102
24. Clegg IM, Everall NJ, King B, Melvin H, Norton C (2001) Appl Spectrosc 55:1138–1150
25. Melendres CA, Narayanasamy A, Maroni VA, Siegel RW (1989) J Mater Res 4:1246
26. Guosheng R, Shouliang W, Panpan WJL, Yunyu C, Zhenfei T, Yixing Y, Changhao L, Guosheng S (2014) RSC Adv 4:63408
27. Baltrus JP, Keller MJ (2019) Surf Sci Spectra 26:014001